

# Targeted metabolomics analysis of three medicinal plants of the genus *Pulsatilla*

Yan-chang Huang<sup>1</sup>, Che Bian<sup>1</sup>, Yu-tong Huang<sup>1</sup>, Wenjuan Hou<sup>1</sup>, Hefei Xue<sup>1</sup>, Yanping Xing<sup>1</sup>, Han Zheng<sup>2,3</sup>, YanYun Yang<sup>1\*</sup>, Tingguo Kang<sup>1</sup> and Liang Xu<sup>1\*</sup>

<sup>1</sup> School of Pharmacy, Liaoning University of Traditional Chinese Medicine, Dalian 116600, China

<sup>2</sup> National Resource Center for Chinese Materia Medica, China Academy of Chinese Medical Sciences, Beijing 100700, China

<sup>3</sup> State Key Laboratory of Dao-di Herbs, Beijing 100700, China

\* Corresponding authors, E-mail: [99yyy@163.com](mailto:99yyy@163.com); [861364054@qq.com](mailto:861364054@qq.com)

## Abstract

*Pulsatilla chinensis*, a member of the Ranunculaceae family, is one of the 12 *Pulsatilla* species distributed in China. During the fruit-ripening period, the achenes of these plants tend to cluster densely in a head-like structure, and the style persists, resembling a silver filament. Resembling an old man with white hair, it is thus named Baitouweng. In this study, *P. chinensis*, *Pulsatilla cernua* (Thunb.) Bercht. & J. Presl, and *Pulsatilla chinensis* var. *kissii* (Mandl) S. H. Li et Y. H. Huan were selected as objects for a detailed targeted metabolomics analysis to determine whether *P. chinensis* var. *kissii* can serve as a substitute for *P. chinensis*-based medicinal materials. A total of 1,558 compounds were identified. Among these, 392 were primary metabolites, 1,166 were secondary metabolites, and 47 were triterpenoid saponins. Clustering analysis of the total metabolites revealed that the three *Pulsatilla* species clustered based on their population origin, rather than their variety. The differential metabolite analysis of triterpenoid saponins showed that metabolic differences between *P. chinensis* var. *kissii* and *P. chinensis* were more pronounced than those between *P. chinensis* var. *kissii* and *P. cernua*. In conclusion, *P. chinensis* var. *kissii* is more suitable as a substitute for *P. cernua* medicinal materials. This result lays a foundation for in-depth investigations into the potential internal relationships among these three *Pulsatilla* species.

**Citation:** Huang Y, Bian C, Huang Y, Hou W, Xue H, et al. 2024. Targeted metabolomics analysis of three medicinal plants of the genus *Pulsatilla*. *Medicinal Plant Biology* 3: e023 <https://doi.org/10.48130/mpb-0024-0025>

## Introduction

*Pulsatilla chinensis* (Bge.) Regel, traditionally known as the Messenger of Hu Wang, old crown flower, or wild father<sup>[1]</sup>, is the only plant from the genus *Pulsatilla* included in the Chinese Pharmacopoeia<sup>[2]</sup>. This traditional Chinese medicine is known for its ability to clear heat, detoxify, cool blood, and stop dysentery. It is commonly used for treating conditions such as heat-induced dysentery, itching, and diarrhea<sup>[2]</sup>. Another plant from the *Pulsatilla* genus, namely *P. cernua*, is one of the few varieties included in the local Chinese medicinal material standards, specifically the Liaoning and Jilin standards<sup>[3,4]</sup>. *P. cernua* is valued for its efficacy in clearing heat and detoxifying, cooling blood, stopping dysentery, relieving pain, stopping bleeding, and eliminating dampness and insects. This medicinal herb is used to treat various symptoms, including heat-induced dysentery, malaria, cold heat, nosebleeds, Yin itching, metrorrhagia, and eczema. *P. chinensis* var. *kissii* was discovered by Karl Mandl during World War I, and in 1922, it was documented in *Österreichische botanische Wochenblatt*, where it was named *Pulsatilla kissii* Mandl<sup>[5]</sup>. Because of its frequent occurrence in the same populations as *P. chinensis* and *P. cernua* and the intermediate length and color of its sepals, Mandl hypothesized that it is a hybrid of *P. chinensis* and *P. cernua*. In China, *P. chinensis* var. *kissii* was discovered in Jinxian County, Dalian City, Liaoning Province, in 1975 and was later incorporated into the Flora of Northeast China. This classification was reaffirmed in the Flora of China (1980 edition)<sup>[6,7]</sup>.

*P. chinensis*, a traditional Chinese medicine, was first documented in the *Shennong Bencao Jing* and has been used in China for thousands of years<sup>[1]</sup>. Triterpenoid saponins are abundantly present in *P. chinensis*, with anemoside B4, anemoside A3, and 23-hydroxybetulinic acid are the primary active ingredients<sup>[8]</sup>. According to the Chinese Pharmacopoeia, the content of anemoside B4 in *P. chinensis* must be > 4.6% for its medicinal effects<sup>[2]</sup>. Anemoside B4 exerts anti-inflammatory<sup>[9]</sup>, antitumor<sup>[10]</sup>, and renal protective<sup>[11]</sup> effects. In the field of research on the identification of plants in the genus *Pulsatilla*, trait identification and microscopic identification have been the primary approaches. Nevertheless, relying solely on the drooping of the calyx before flowering and the color of the calyx lobes as identification characteristics is not sufficient for trait identification. On the contrary, the apparent characteristics and microscopic features of leaves can be regarded as reliable traits for identifying plants in the genus *Pulsatilla*<sup>[12]</sup>. A comparative study of triterpenoid compounds in *P. chinensis* and *P. cernua* revealed that lupane-type compounds are more abundant in *P. chinensis*, while oleanane-type compounds are more abundant in *P. cernua*<sup>[13]</sup>. Simultaneously, molecular identification methods such as DNA barcoding and PCR-RFLP have facilitated accurate delineation of the adulterants of plants within the genus *Pulsatilla* and other genera<sup>[12,14]</sup>. Digital research on traditional Chinese medicine is a new hotspot. Digitization of liquid mass spectrometry results of *P. chinensis* and *P. cernua*<sup>[15]</sup> provides a new direction for research on the identification of plants within

the same genus. In addition, our previous study on the phylogeny of plants in the genus *Pulsatilla* revealed that *P. chinensis*, *P. chinensis* var. *kissii*, and *P. chinensis* f. *alba* converge into a single branch, with *P. cernua* and other *Pulsatilla* species diverging to form a separate branch<sup>[16]</sup>.

According to a review of literature on plants in the genus *Pulsatilla*, most studies have focused on traditional medicinal applications<sup>[17]</sup>, individual active components, and their pharmacological effects<sup>[18–21]</sup>. However, because medicinal plants contain multiple chemical components, the efficacy of a single compound is often limited, and relying on a single component cannot serve as the standard for identifying alternative medicinal plants. In recent years, with the advancement of metabolomics analysis, studies on the differences within and among species of the same genus<sup>[22–25]</sup> have become increasingly comprehensive, offering valuable insights into the alternative medicinal materials within the genus *Pulsatilla*. To explore the potential of *P. chinensis* var. *kissii* as a medicinal herb, ultra-performance liquid chromatography-tandem mass spectrometry (UPLC–MS/MS) was conducted for a targeted metabolomics analysis on *P. chinensis*, *P. chinensis* var. *kissii*, and *P. cernua*. This study examined differential metabolites in these three species, focusing specifically on differences in the triterpenoid saponin components. Based on the analysis results, it was assessed whether *P. chinensis* var. *kissii* is more closely related to *P. chinensis* or *P. cernua*.

## Materials and methods

### Plant material

Three *Pulsatilla* species, namely *P. chinensis*, *P. cernua*, and *P. chinensis* var. *kissii*, were selected (Supplementary Fig. S1). In May 2023, during the fruit-ripening period, the underground parts of the three *Pulsatilla* species were collected for the experiments from three sites in China: Qianshan Mountain in Anshan City, the mountain east of Dalian University, and Daheishan Mountain. The three types of *Pulsatilla* were identified by Professor Xu Liang from Liaoning University of Traditional Chinese Medicine. Widely distributed in Northeast China, these varieties require no permit for collection. Voucher specimens *P. chinensis* (No. 2010023517005-2), *P. chinensis* var. *kissii* (No. 2010023517014-2), and *P. cernua* (No. 2010023517003) are deposited in the Teaching and Research Section of Chinese Medicinal Plant Cultivation and Identification, School of Pharmacy, Liaoning University of Traditional Chinese Medicine.

### Reagents

Methanol and acetonitrile (chromatographically pure, Merck Drugs and Biotechnology) and formic acid (chromatographically pure, Shanghai Aladdin Biochemical Technology Co., Ltd., Shanghai, China) were used as reagents.

### Instruments

An ordinary silicone oil heating freeze-drying machine (Scientz-100F, Ningbo Scientz Biotechnology Co., Ltd., Ningbo, Zhejiang, China), a freeze mixing ball mill (MM 400, Verder Shanghai Instrument and Equipment Co., Ltd.), a hundred-thousandth electronic balance (AS 60/220.R2 RADWAG, Poland), a desktop high-speed freezing microcentrifuge (D3024, Dalong Xingchuang Experimental Instrument (Beijing) Co., Ltd., Beijing, China), an ultra-high-performance liquid

chromatography system (ExionLC AD, SCIEX, USA), and a tandem mass spectrometer (Applied Biosystems 4500QTRAP, Applied Biosystems, USA) were the main equipment used in this study.

### Preparation and extraction of samples

One sample each of *P. chinensis*, *P. chinensis* var. *kissii*, and *P. cernua* were collected from each production area, totaling nine samples. The sample powders were stored in a  $-80^{\circ}\text{C}$  refrigerator before metabolite extraction. For the extraction process, 50 mg of the sample powder was weighed using an electronic balance (AS 60/220.R2). To this, 1,200  $\mu\text{L}$  of 70% methanol–water internal standard extract, precooled at  $-20^{\circ}\text{C}$ , was added. The mixture was vortexed every 30 min for 30 s, 6 times. The samples were then centrifuged at 12,000 rpm for 3 min, and the supernatant was obtained. The extracted supernatant was filtered using a microporous filter membrane with a pore size of 0.22  $\mu\text{m}$  and stored in an injection vial for UPLC–MS/MS analysis.

### Collection conditions for chromatography and mass spectrometry

The data acquisition system primarily consisted of UPLC (ExionLC AD, <https://sciex.com.cn/>) and tandem mass spectrometry (MS/MS).

### Liquid chromatography conditions

For the liquid-phase conditions, an Agilent SB-C18 1.8  $\mu\text{m}$ , 2.1 mm  $\times$  100 mm column was used. The mobile phases consisted of Phase A, comprising ultrapure water with 0.1% formic acid, and Phase B, comprising acetonitrile with 0.1% formic acid. The mobile phase elution gradient was programmed as follows: starting with 5% Phase B at 0.00 min, the proportion of Phase B was increased linearly to 95% over 9.00 min. This 95% B-phase was maintained for 1 min. From 10.00 to 11.10 min, the B-phase proportion was reduced back to 5% and then equilibrated at 5% for 14 min. The flow rate was set at 0.35 mL/min, and the column temperature and the injection volume were set to  $40^{\circ}\text{C}$  and 2  $\mu\text{L}$ , respectively. The effluent was alternately connected to an ESI-triple quadrupole linear ion trap-MS for analysis.

### Mass spectrometry conditions

The electrospray ionization (ESI) temperature was set to  $550^{\circ}\text{C}$ , with the ion spray voltage of 5,500 V in the positive ion mode and  $-4,500$  V in the negative ion mode. The pressures of ion source gases I and II and curtain gas were set to 50, 60, and 25 psi, respectively. The collision-induced ionization parameters were set to high. QQQ (Applied Biosystems 4500QTRAP, Applied Biosystems, USA) scans were performed in the multi-response monitoring (MRM) mode, with the collision gas (nitrogen) set to medium. The declustering potential (DP) and collision energy (CE) were further optimized for individual MRM ion pairs (Supplementary Table S1). A specific set of MRM ion pairs was monitored in each period based on the metabolites that eluted during that period.

### Analysis of quality control samples

Quality control (QC) samples were prepared by mixing sample extracts to analyze the repeatability of sample analysis under the same treatment conditions. During the instrument analysis process, generally, one QC sample is inserted for every 10 detected and analyzed samples to monitor the repeatability of the analysis process. Based on the overlapping between the

## Metabolomics analysis

total ion current (TIC) diagrams of mass spectrometry detection and analysis of different QC samples (Supplementary Fig. S2), the repeatability of metabolite extraction and detection, that is, the feasibility of technical repetition, can be judged.

### Coefficient of variations of the samples

The coefficient of variation (CV) is the ratio of the standard deviation of the original data to the mean of the original data, and it is an indicator of the degree of data dispersion. The empirical cumulative distribution function (ECDF) can be used to analyze the frequency of occurrence of substances with CVs lower than the reference value. In a QC sample, a higher proportion of substances with low CVs implies greater stability of the experimental data. In the present study, the proportion of substances with CV values  $< 0.5$  was  $> 85\%$ , which indicated the stability of the experimental data. Moreover, the proportion of substances with CV values  $< 0.3$  in the QC samples was more than  $75\%$ , which confirmed that the experimental data were highly stable (Supplementary Fig. S3).

### Qualitative and quantitative analyses of metabolites

Based on a self-built database, Metware (MWDB), a qualitative analysis was performed according to the secondary spectrum information. During the analysis, the isotope signals, duplicate signals containing  $K^+$ ,  $Na^+$ , and  $NH_4^+$ , and duplicate signals of fragment ions that are fragments of substances with larger molecular weights were removed (Supplementary Table S2).

Metabolite quantification was completed through triple quadrupole mass spectrometry in the MRM mode (Supplementary Fig. S4). In the MRM mode, the quadrupole first screens the precursor ion (parent ion) of the target substance and excludes ions corresponding to substances with other molecular weights to initially eliminate interference; after the precursor ion is fragmented through collision-induced ionization in the collision chamber to form many fragment ions, the fragment ions are filtered through the triple quadrupole to select a required characteristic fragment ion, excluding non-target ion interference to ensure the accuracy and repeatability of the quantitative analysis. Mass spectrometry data were processed using software Analyst 1.6.3. The TIC chromatogram (Supplementary Fig. S5a & b) and the MRM metabolite detection multi-peak chromatogram (ion current chromatogram extracted from multiple substances, XIC) (Supplementary Fig. S6a & b) of the QC samples were obtained.

Based on the local metabolic database, qualitative and quantitative mass spectrometry analyses were performed on the sample metabolites. The multi-peak diagram of metabolite detection in the MRM mode shows the substances detected in the sample, with each metabolite represented by separate chromatographic peaks of different colors. The characteristic ions of each substance were screened through triple quadrupole, and the signal intensity (count per second, CPS) of the characteristic ions was obtained in the detector. The mass spectrometry file of the sample was opened using MultiQuant software for the integration and correction of chromatographic peaks. The peak area (Area) of each chromatographic peak represents the relative content of the corresponding substance. Finally, integration data for the chromatographic peak area were exported and saved.

To compare differences in the metabolite content among different samples, according to the information on metabolite

retention time and peak shape, the chromatographic peaks of each metabolite detected in the samples were corrected, thereby ensuring the accuracy of the qualitative and quantitative analysis results. Supplementary Fig. S7 shows the integrated and corrected results of the quantitative analysis for randomly selected metabolites in the samples. The abscissa is the retention time (min) of metabolite detection, and the ordinate is the ion current intensity (cps) of a certain metabolite ion detection.

### Statistical analysis

Principal component analysis (PCA) is a multidimensional statistical method used for unsupervised pattern recognition. In this study, PCA was performed using the built-in statistical prcomp function in R software ([www.r-project.org](http://www.r-project.org)), version 3.5.1 (base package). The prcomp function was set with the parameter `scale = true` to apply unit variance scaling to the data.

Orthogonal partial least squares discriminant analysis (OPLS-DA) combines orthogonal signal correction with PLS-DA methods, allowing the decomposition of the X matrix into the information correlated and uncorrelated with Y. This process enables the screening of differential variables by removing uncorrelated differences. For OPLS-DA, the data were  $\log_2$ -transformed and then centralized (Supplementary Fig. S8). Here, X represents the quantitative information matrix of the samples, whereas Y denotes the grouping information matrix of the samples. The analysis was performed using MetaboAnalystR 1.0.1 and the OPLSR function in R software.

### Hierarchical cluster analysis

Cluster analysis (CA) is a multivariate statistical method used for categorization, where individuals or samples are grouped based on their characteristics. The goal is to maximize homogeneity within each category as well as between different categories. CA is primarily used in exploratory studies, and its analysis can yield multiple potential solutions. The selection of the final solution often requires the researcher's subjective judgment and further analysis. In this study, metabolite content data were processed using unit variance (UV) scaling, and heatmaps were generated using the R software package ComplexHeatmap 2.8.0. The accumulation patterns of the metabolites across different samples were then analyzed using hierarchical CA.

### Differential metabolite analysis

The metabolites that were significantly regulated between the two groups were identified based on a variable importance in projection (VIP) value of  $\geq 1$  and an absolute  $\log_2FC$  (fold change) of  $\geq 1$ . The VIP value was extracted from the OPLS-DA results, which also included a rating chart and a permutation chart, generated using an R package MetaboAnalystR. Before OPLS-DA, the data were logarithmically transformed ( $\log_2$ ) and mean-centered. To avoid overfitting, permutation tests were performed with 200 iterations.

### KEGG annotation and enrichment analysis

The identified metabolites were annotated using the Kyoto Encyclopedia of Genes and Genomes (KEGG) compound database ([www.kegg.jp/kegg/compound](http://www.kegg.jp/kegg/compound)) and mapped to the KEGG pathway database ([www.kegg.jp/kegg/pathway](http://www.kegg.jp/kegg/pathway)). Pathways identified to significantly regulate metabolites were then input into the metabolite set enrichment analysis, and their

significance was determined through  $p$  values derived from hypergeometric tests.

### Evaluation of repeatability correlation.

The correlation analysis between samples can be used to observe the biological replicates between samples within a group. At the same time, the higher the correlation coefficient between samples within a group relative to samples between groups, the more reliable the obtained differential metabolites are. The Pearson correlation coefficient  $r$  (Pearson's Correlation Coefficient) is used as an evaluation index for biological repeatability correlation. The Pearson correlation coefficient is calculated using the built-in `cor` function of R software. The closer  $|r|$  is to 1, the stronger the correlation between two repeated samples (Supplementary Fig. S9, Supplementary Tables S3 & S4).

## Results

### Analysis of total metabolites in three types of *Pulsatilla* medicinal herbs

*P. chinensis* has been documented in medicinal texts since the *Shen Nong Ben Cao Jing* and has historically been the mainstream medicinal variety. *P. cernua* is recorded in the medicinal diagrams of the Japanese herbal text *Ben Cao Tu Pu*, written during the Ming and Qing dynasties. Additionally, it is listed in the Chinese herbal medicine standards of Jilin and Liaoning provinces, where it is used similarly to *P. chinensis*. *P. chinensis* var. *kissii*, a variant of *P. chinensis* commonly found and used locally in Dalian, Anshan, and Liaoyang cities in Liaoning province. Its distribution overlaps significantly with that of *P. chinensis* and *P. cernua* in Liaoning province, often leading to cases of mistaken harvesting and misuse in the wild. To better understand the medicinal value of *P. chinensis* var. *kissii* and compare its metabolites with those of the other two recorded medicinal *Pulsatilla* species, extensive targeted metabolite analysis was conducted using UPLC–MS/MS. A total of 1,558 metabolites were identified. In the negative ion mode, four ion modes were used, including  $[M-H]^-$ ,  $[M+CH_3COO]^-$ ,  $[M-Na]^-$ , and  $[M+CH_3COOH-H]^-$ . A total of 748 metabolites, encompassing 143 primary metabolites and 605 secondary metabolites, were detected. Fifteen triterpenoid saponin components, including pulsatilloside C, anemoside B4, anemoside A3, pulsatilla saponin D, and hederacoside D, were identified and found to be distributed across all three types of *Pulsatilla* medicinal herbs. In the positive ion mode, six ion modes were used, including  $[M+H]^+$ ,  $[M]^+$ ,  $[M+NH_4]^+$ ,  $[M-H_2O+Na]^+$ ,  $[M+Na]^+$ , and  $[M-H_2O+H]^+$ . A total of 810 metabolites, encompassing 249 primary metabolites and 561 secondary metabolites, were detected. Thirty-two triterpenoid saponin components were identified in the positive ion mode, including hederacoside C, dipsacoside B, mutong saponin A, and kalopanaxsaponin H, all of which were distributed across the three *Pulsatilla* medicinal herbs.

A comparison of the metabolite detection results of the three *Pulsatilla* medicinal herbs revealed several unique metabolites in *P. chinensis* var. *kissii*, *P. chinensis*, and *P. cernua*. Specifically, quercetin 3-*O*-apiryl (1→2) galactoside, 3',5',5,7-tetrahydroxy-4'-methoxyflavonone-3'-*O*-glucoside, 3-*O*-ferulic acid quinic acid (a phenolic acid), and guanidine (an alkaloid) were present in *P. chinensis* var. *kissii* but not in the other two types of

*Pulsatilla* within the same population. In addition, the triterpenoid saponins 3-*O*-rhamnosyl (1→2) arabinose glycosyl-28-*O*-glucoside and ivy saponin-3-*O*- $\alpha$ -L-rhamnose (1→2)-( $\beta$ -D-glucose group (1→4))- $\alpha$ -L-arabinose, as well as the flavonoids tamarixin, paeonol neoglycoside, peony glycoside, and 2,5-dimethyl-7-hydroxychromone glucoside, were unique to *P. chinensis*. Unique metabolites in *P. cernua* included the phenolic acid salvianolic acid I, hairy flower glycoside, and alkaloid isocyanidin. These unique metabolites can facilitate the differentiation between the three species of *Pulsatilla*. Using the 1,558 detected metabolites, a CA was performed on the nine samples representing the three types of *Pulsatilla*. The results indicated that the growth environment affected the overall clustering of metabolites. *Pulsatilla* samples of the same variety did not cluster together, whereas those of different *Pulsatilla* varieties from the same population tended to cluster together. These results are illustrated in Fig. 1.

### Multivariate analysis of identified metabolites

To investigate differences in metabolite contents among the three types of *Pulsatilla* medicinal herbs, particularly between *P. chinensis* var. *kissii* and the other two types of *P. chinensis*, PCA was conducted on the data from 1,558 metabolites. The PCA results revealed that the three *Pulsatilla* medicinal herbs clustered together, with the model variance explained by the PCA 1 and PCA 2 axis being 39.72% (Fig. 2). The metabolomic differences along the PCA1 axis among the three *Pulsatilla* species were not significant. This analysis highlighted the correlation between the metabolite profiles of the three groups and varieties of *Pulsatilla*.

To further analyze and determine differences in the metabolite composition among samples within the group, supervised orthogonal signal correction combined with partial least squares discriminant analysis (OPLS-DA) was used for better differentiation between the groups, as shown in Fig. 3. In this study, the OPLS-DA model was used to compare the metabolite content of paired samples and evaluate the relationships between *P. chinensis* var. *kissii* and *P. chinensis* ( $R^2X = 0.469$ ,  $R^2Y = 0.997$ ,  $Q^2 = 0.492$ ); *P. chinensis* var. *kissii* and *P. cernua* ( $R^2X = 0.392$ ,  $R^2Y = 0.999$ ,  $Q^2 = 0.429$ ); and *P. cernua* and *P. chinensis* ( $R^2X = 0.468$ ,  $R^2Y = 0.993$ ,  $Q^2 = 0.468$ ).

### CA of differential metabolites in the three medicinal herbs of the genus *Pulsatilla*

Using the differential metabolites identified in OPLS-DA, a CA was performed on the three types of *Pulsatilla* medicinal herbs. The analysis revealed that triterpenoid saponin components, such as anemoside B4, were present in higher concentrations in *P. chinensis* than in the other two herb types. The results of this analysis are presented in Fig. 4.

### Analysis of differential metabolites between *P. chinensis* and *P. chinensis* var. *kissii*

Based on the t-test results with  $p$  values < 0.05 and variable importance (VIP) values  $\geq 1.0$ , a total of 278 significantly different metabolites were identified between *P. chinensis* var. *kissii* and *P. chinensis*. Among these, the contents of 192 metabolites were higher in *P. chinensis* var. *kissii* than in *P. chinensis*, whereas those of 86 metabolites were lower in *P. chinensis* var. *kissii*. The 278 different metabolites were classified into 12 categories, with terpenoids being the most represented (65 metabolites), followed by phenolic compounds (60 metabolites). Among the differential metabolites in the terpenoid category, 28 were

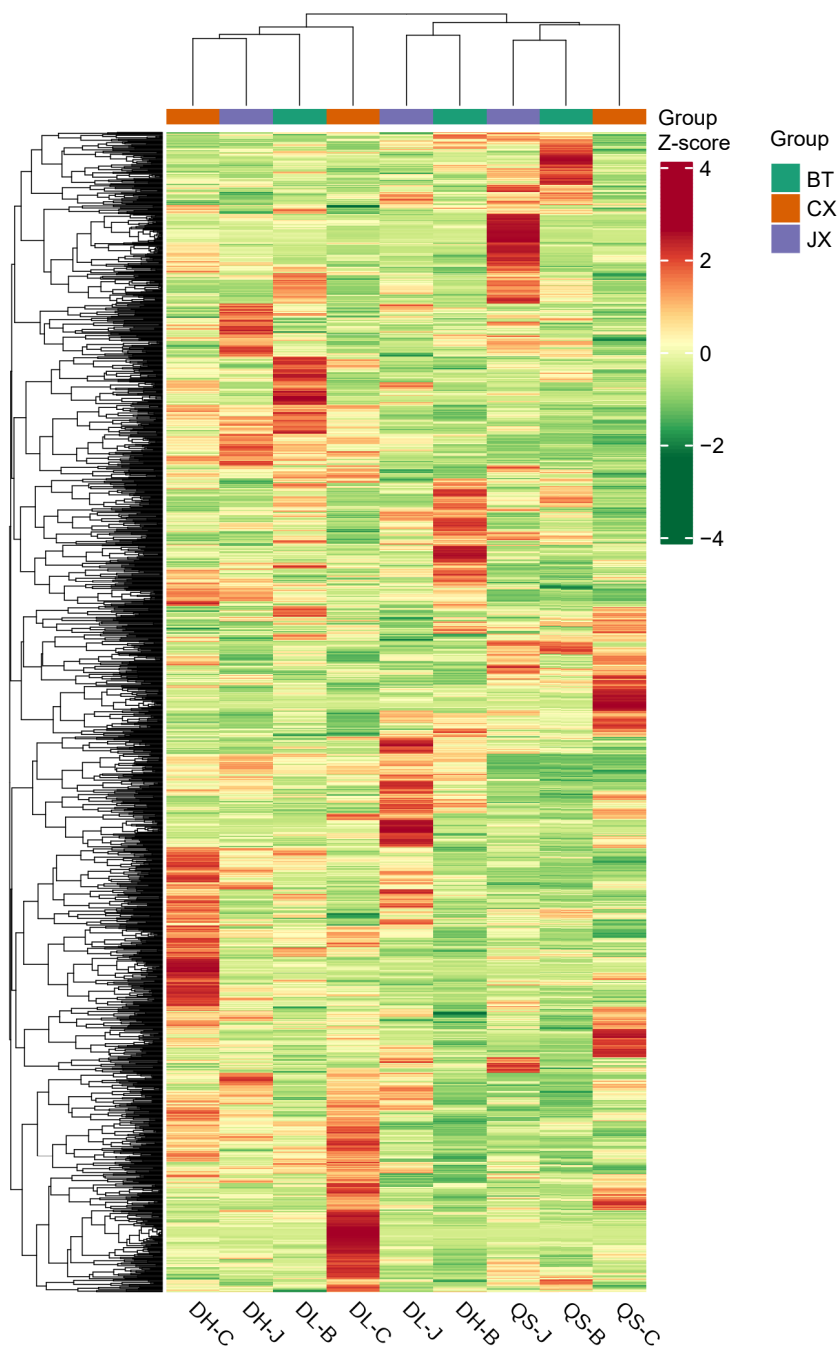


**Fig. 1** Cluster analysis of the total metabolic products of *P. chinensis*, *P. cernua*, and *P. chinensis* var. *kissii*. BT (B): *P. chinensis*; CX (C): *P. cernua*; and JX (J): *P. chinensis* var. *kissii*. DH: Daheishan Mountain; DL: the mountain east of Dalian University; and QS: Qianshan Mountain in Anshan City.

triterpenoid saponins. Of these, 10 compounds were upregulated in *P. chinensis* var. *kissii*, most of which are pentacyclic triterpenoid compounds of the oleanolic acid type, such as oleanol-3-*O*-glucoside, oleanol-3-*O*-glucosyl (1-2) glucoside, and dipsacussaponin B. By contrast, 18 compounds were downregulated, with the contents of saponin compounds such as anemoside A3, anemoside B4, and anemoside C being lower in *P. chinensis* var. *kissii* than in *P. chinensis*. In addition, hederacoside C and hederacoside D were significantly downregulated in *P. chinensis* var. *kissii*. The results are illustrated in Fig. 5.

### Analysis of differential metabolites between the medicinal materials of *P. chinensis* var. *kissii* and *P. cernua*

Based on the t-test results, with  $p$  values < 0.05 and VIP values  $\geq 1.0$ , a total of 304 significantly different metabolites were identified in the comparison between *P. chinensis* var. *kissii* and *P. cernua*. Among these, the contents of 165 metabolites were higher and those of 139 metabolites were lower in *P. chinensis* var. *kissii* than in *P. cernua*. The 304 metabolites were classified into 12 categories, with terpenoids accounting for the largest proportion (66 metabolites), followed by phenolic acids

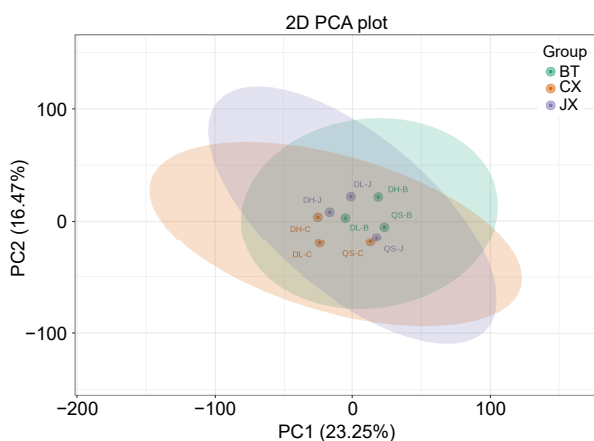


**Fig. 2** Principal component analysis of the overall metabolites of the three types of *Pulsatilla* medicinal materials (BT: *P. chinensis*. CX: *P. cernua*. JX: *P. chinensis* var. *kissii*).

(42 metabolites). Within the terpenoid category, 20 triterpenoid saponin compounds exhibited differential expression. Of these, 13 compounds were upregulated in *P. chinensis* var. *kissii*, most of which were anemoside compounds, namely anemoside A3, anemoside B4, and anemoside C, with signifi-

cant upregulation compared with *P. cernua*. In addition, Yusaponin I and mutongsaponins from other regions were upregulated. Conversely, seven compounds were downregulated, including dipsacoside B, Udosaponin A methyl ester, and hederacoside D; all these compounds exhibited significant downregulation compared with that in *P. cernua*. The results are presented in Fig. 6.

### Analysis of differential metabolites between *P. cernua* and *P. chinensis*

Based on the t-test results, with  $p$  values  $< 0.05$  and VIP values  $\geq 1.0$ , a total of 400 significantly different metabolites were identified between *P. cernua* and *P. chinensis*. Among these, the contents of 231 metabolites were higher in *P. cernua* than in *P. chinensis*, whereas those of 169 metabolites were lower in *P. cernua*. The 394 metabolites were classified into 12 categories, with terpenes accounting for the largest proportion (89 metabolites), followed by phenolic compounds (76 metabolites). In the terpenoid category, 32 triterpenoid saponin compounds exhibited differential expression. Of these, 13 compounds, including dipsacoside B, dipsacussaponin B, oleanol-3-O-glucoside, and anemoside D, were upregulated in *P. cernua*. Conversely, 19 compounds, including anemoside A3, anemoside B4, and anemoside C, were downregulated in *P. cernua*. The results are presented in Fig. 7.

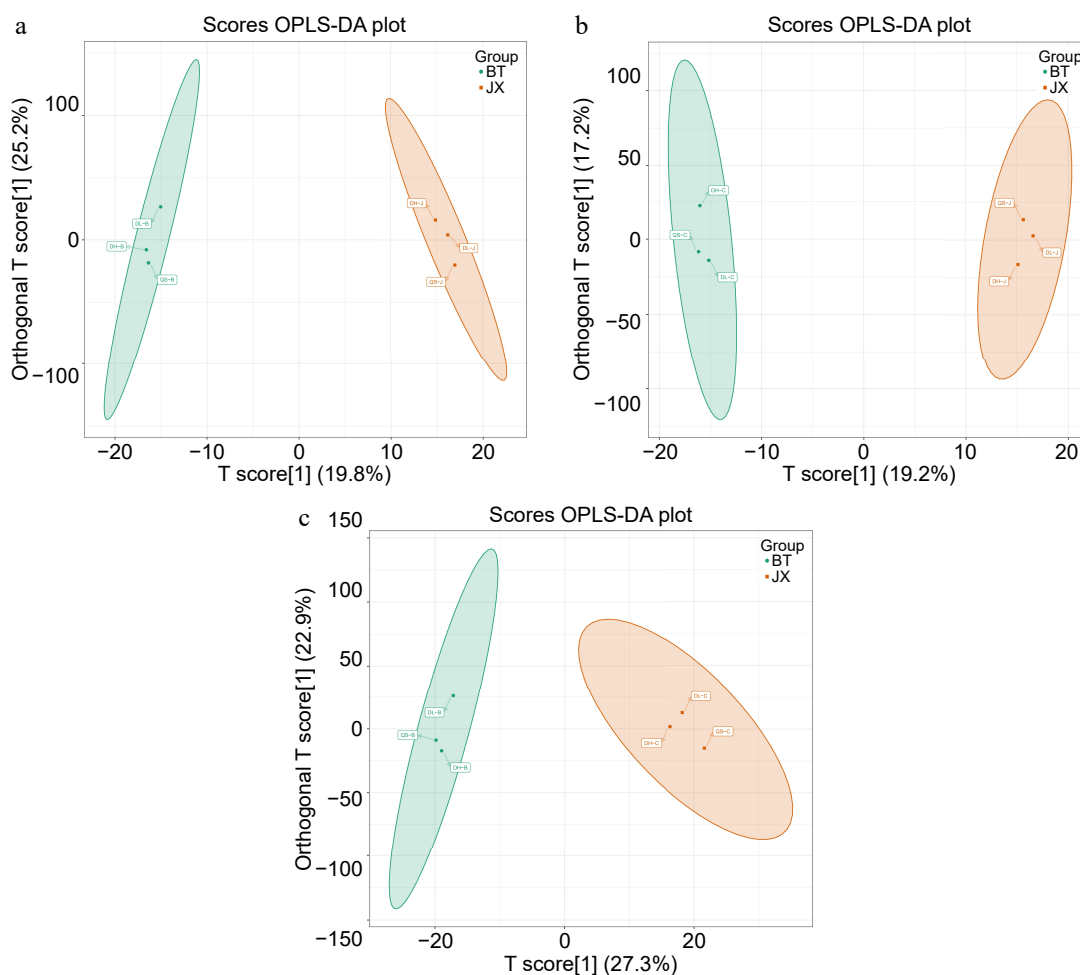


**Fig. 3** OPLS-DA score plots of the three types of *Pulsatilla* medicinal materials. (a) *P. chinensis* var. *kissii* and *P. chinensis*; (b) *P. chinensis* var. *kissii* and *P. cernua*; (c) *P. cernua* and *P. chinensis*.

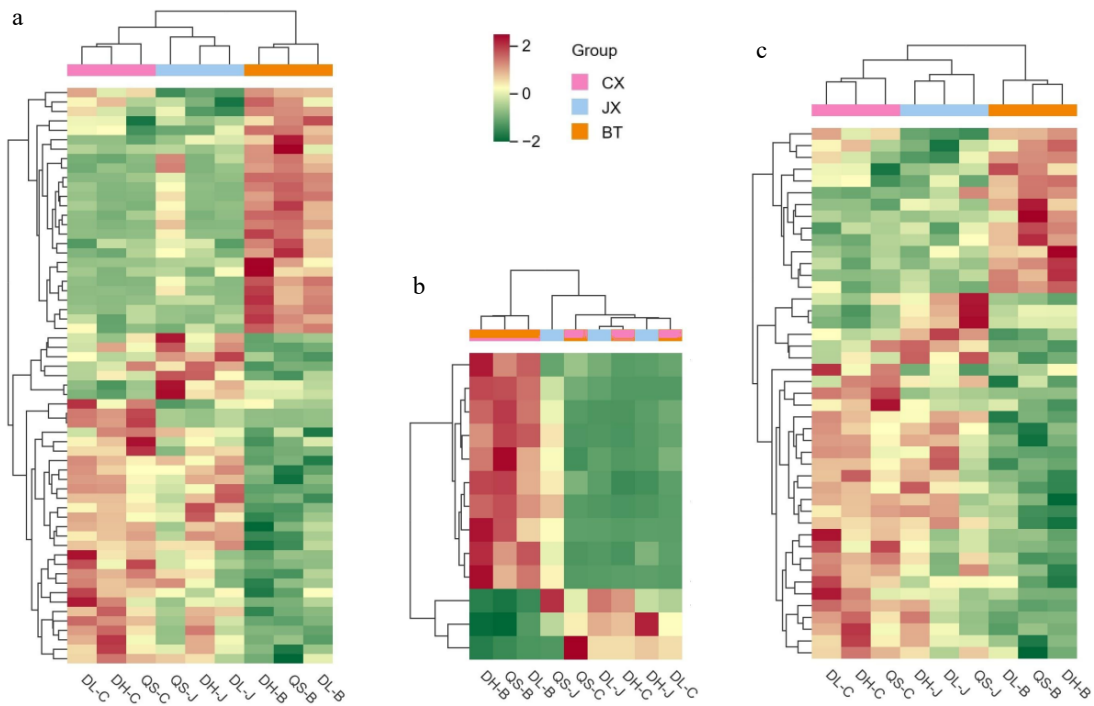


**Fig. 4** Cluster diagram of differential metabolites present in three types of *Pulsatilla* medicinal materials. (a) Total differential metabolites; (b) differential metabolites of triterpenoid saponin components; (c) differential metabolites of nontriterpenoid saponin components.

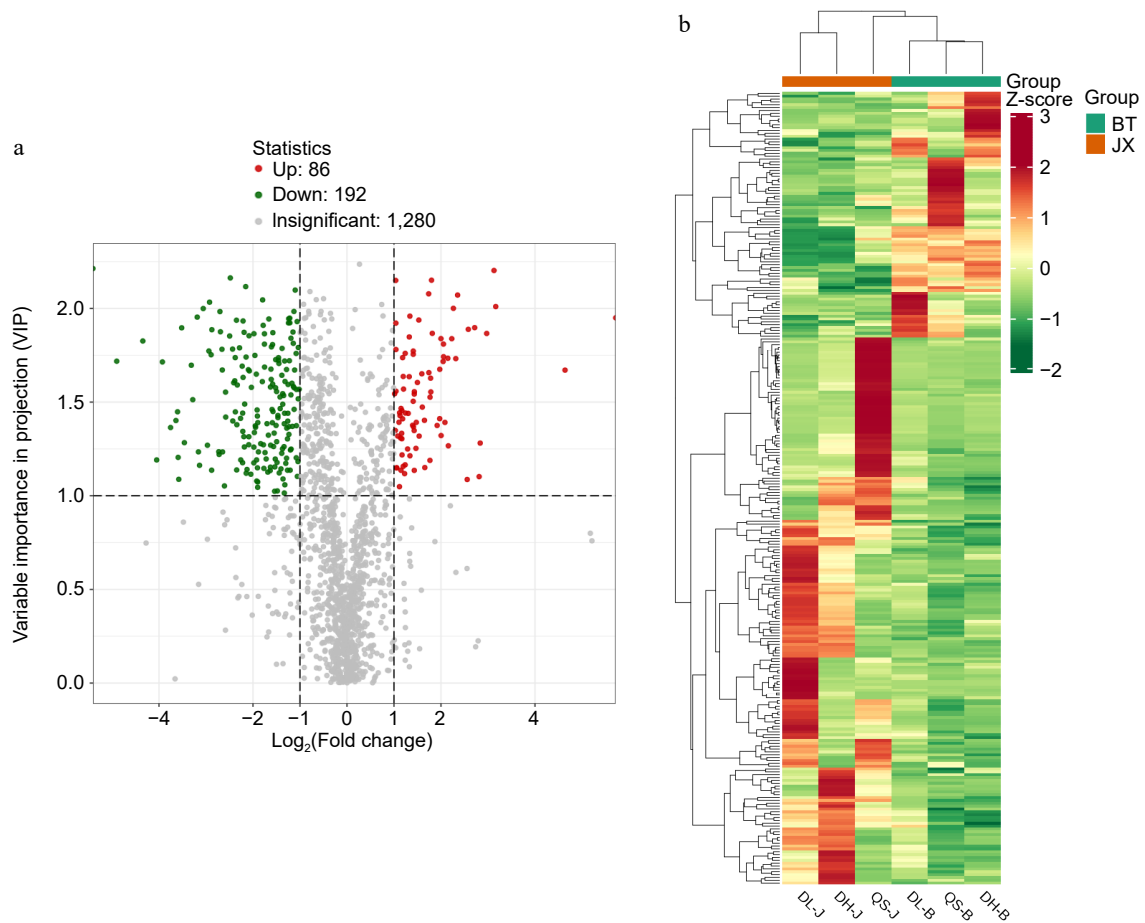


**Fig. 5** (a) Volcano plot of differential metabolites between *P. chinensis* var. *kissii* and *P. chinensis*; red and green colors represent the numbers of metabolites with significant differences among the metabolites. Upregulated metabolites are depicted in red, whereas downregulated metabolites are shown in green. (b) Cluster heatmap of differential metabolites between *P. chinensis* var. *kissii* and *P. chinensis*.

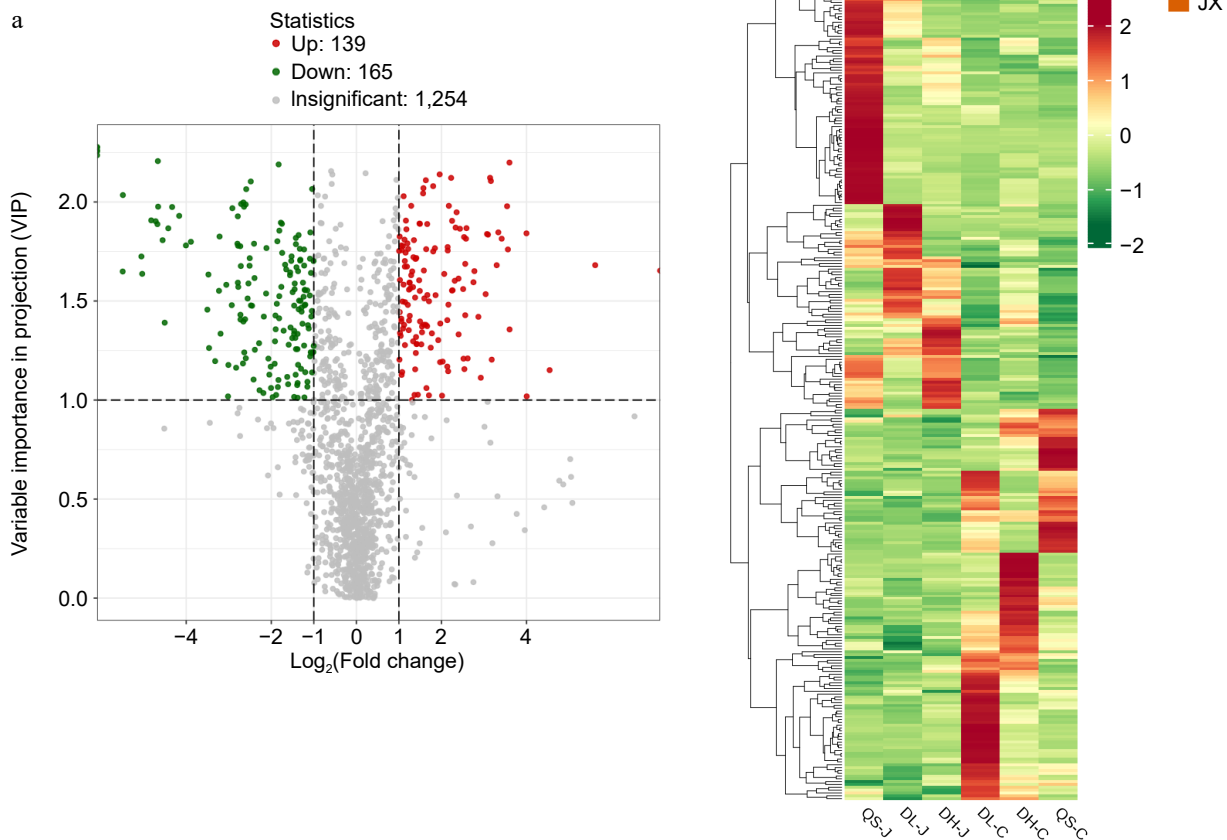


**Fig. 6** (a) Volcano plot of differential metabolites between *P. chinensis* var. *kissii* and *P. cernua*. (b) Cluster heatmap of differential metabolites between *P. chinensis* var. *kissii* and *P. cernua*.

### KEGG pathway enrichment analysis of differential metabolites

KEGG pathway enrichment analysis was conducted to determine differences in the metabolic pathways between the groups *P. chinensis* var. *kissii* and *P. chinensis*. The KEGG database is a valuable resource that allows researchers to study genes, gene expression profiles, and metabolite content within an integrated network. As the primary public database related to pathways, KEGG provides queries for various metabolic pathways, including the metabolism of carbohydrates, nucleotides, amino acids, and the biodegradation of organic matter. It not only outlines all possible metabolic pathways but also provides comprehensive annotations of the enzymes catalyzing each step, including amino acid sequences and Protein Data Bank (PDB) library links. These functions make the KEGG database a powerful tool for metabolic analysis and metabolic network research in different organisms. Based on the differential metabolites identified, we conducted the KEGG pathway enrichment analysis. The rich factor is defined as the ratio of the number of differential metabolites in a given pathway to the total number of metabolites annotated in that pathway; the higher the rich factor, the greater the degree of enrichment. Moreover, *p* values determined using a hypergeometric test

indicated the significance of the enrichment (Supplementary Fig. S10). The closer the *p*-value is to 0, the more significant the enrichment. The size of the dots in the figure represents the number of differential metabolites in each pathway. For clarity, the top 20 pathways selected based on *p* values have been displayed.

### KEGG analysis of differential metabolites between *P. chinensis* var. *kissii* and *P. chinensis*

The KEGG classification of differential metabolites revealed that the most enriched pathways between the groups *P. chinensis* var. *kissii* and *P. chinensis* were flavonoid biosynthesis, tyrosine metabolism, and isoquinoline alkaloid biosynthesis. In the flavonoid biosynthesis pathway, five differential metabolites, including trans-5-*O*-*p*-coumaryl shikimic acid (a phenolic acid), and flavonoids, such as curcumin, quercetin, catechins, and dihydroquercetin, were identified. The tyrosine metabolism pathway featured four differential metabolites: the phenolic acids danshensu, para-coumaric acid, and rosmarinic acid, as well as the amino acid derivative levodopa. In the isoquinoline alkaloid biosynthesis pathway, three differential metabolites were identified: *p*-coumaric acid (a phenolic acid), tetrandrine (an alkaloid), and levodopa (an amino acid derivative). The pathway with the highest number of differential



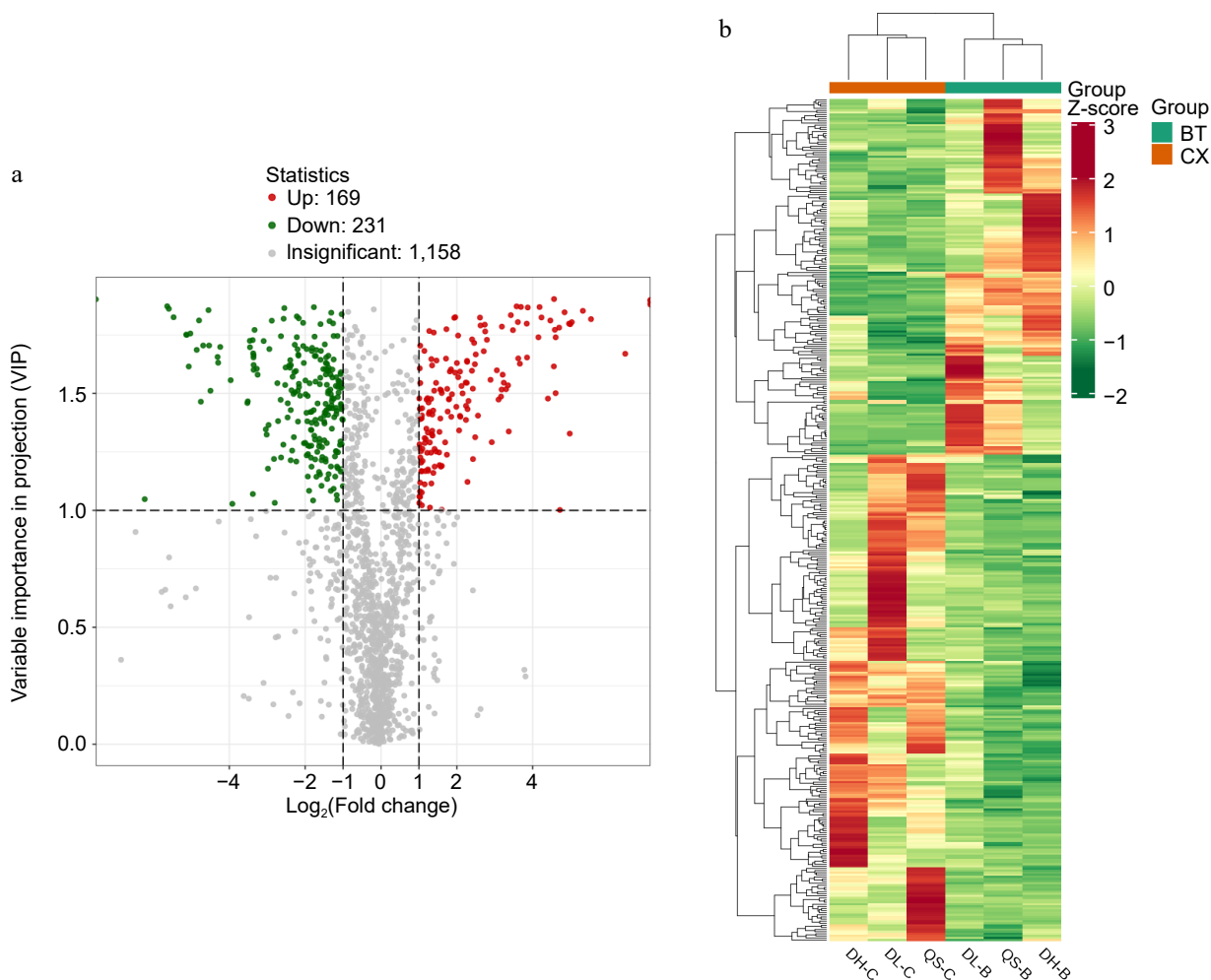


**Fig. 7** (a) Volcano plot of differential metabolites between *P. chinensis* and *P. cernua*. (b) Cluster heatmap of differential metabolites between *P. chinensis* and *P. cernua*.

metabolites was the biosynthesis of secondary metabolites, including a total of 19 differential metabolites. These metabolites belonged to various categories, including amino acids and derivatives, lipids, phenolic acids, terpenes, organic acids, flavonoids, and alkaloids (Supplementary Fig. S11).

### KEGG analysis of different metabolites in medicinal materials of *P. chinensis* var. *kissii* and *P. cernua*

The KEGG classification of differential metabolites revealed that the differential metabolites between *P. chinensis* var. *kissii* and *P. cernua* were most significantly enriched in the flavonoid biosynthesis and plant hormone signaling pathways. In the flavonoid biosynthesis pathway, seven differential metabolites were identified, including 5-*O*-coumaric acid (a phenolic acid), galangin, quercetin, catechin, apigenin, dihydroquercetin, and dihydroquercetin in flavonoids. The plant hormone signaling pathway featured three differential metabolites: jasmonic acid and abscisic acid (organic acids) and jasmonic acid-*L*-isoleucine (an amino acid derivative). The pathway with the highest number of differential metabolites was the biosynthesis of secondary metabolites, with a total of 25 differential metabolites identified. These metabolites belonged to various categories, including amino acids and derivatives, lipids, nucleic

acids and their derivatives, lignans and coumarins, phenolic acids, terpenes, organic acids, flavonoids, and alkaloids (Supplementary Fig. S12).

### KEGG analysis of differential metabolites between *P. cernua* and *P. chinensis*

The KEGG classification of differential metabolites revealed that the most significant enrichment between *P. chinensis* and *P. cernua* groups occurred in the flavonoid biosynthesis and ascorbic acid and aldehyde metabolism pathways. In the flavonoid biosynthesis pathway, seven differential metabolites were identified, including trans-5-*O*-*p*-coumaroyl shikimic acid and chlorogenic acid (3-*O*-caffeoyl quinic acid) from the phenolic acids category, as well as quercetin, gallic acid, naringenin, apigenin-8-*C*-glucoside, and dihydroquercetin from the flavonoids category. In the ascorbic acid and aldehyde metabolism pathway, arachidonic acid (a lipid) was identified as a differential metabolite. The pathway with the highest number of differential metabolites was the biosynthesis of secondary metabolites, with a total of 26 differential metabolites identified. These metabolites belonged to various categories, including amino acids and derivatives, lipids, nucleic acids and their derivatives, lignans and coumarins, phenolic acids, terpenes, organic acids, flavonoids, and alkaloids (Supplementary Fig. S13).

## Discussion

Previous studies based on the clustering heatmap of metabolites, medicinal plants of the same genus but different species have been consistently grouped together<sup>[26,27]</sup>. However, the results of the present analysis of the three types of *Pulsatilla* medicinal materials are inconsistent with this prediction. It was anticipated that the total metabolites of the three types of *Pulsatilla* would cluster by species, leading to the grouping of the same species. Instead, clustering of different species of *Pulsatilla* from the same geographic origin were noted. This outcome is likely influenced by the origin, climate, and other environmental conditions of the three types of *Pulsatilla* medicinal materials. Therefore, it is concluded that the effect of environmental factors<sup>[28]</sup> on the content of total metabolites is more pronounced than that of interspecies differences in the case where medicinal plants belong to the same genus but different species are distributed in a single area (such as Liaoning Province) but exposed to different environments.

In the analysis of differential metabolites identified across the three types of *Pulsatilla* species, it was observed that the clustering heatmaps for the total differential metabolites, triterpenoid saponins, and nontriterpenoid saponins of *P. chinensis* exhibited significant dissimilarities compared with those of *P. cernua* and *P. chinensis* var. *kissii*. Conversely, the results for *P. cernua* and *P. chinensis* var. *kissii* were highly consistent, particularly in the clustering of triterpenoid saponins, where *P. chinensis* and *P. chinensis* var. *kissii* did not cluster together by species. Moreover, the volcano plot results for the three types of *Pulsatilla* indicated that the main active compounds of *P. chinensis*, including anemoside B4, anemoside A3, and anemoside C, were downregulated in the comparison between *P. chinensis* var. *kissii* and *P. chinensis* but upregulated in the comparison between *P. chinensis* var. *kissii* and *P. cernua*. Based on these results, it is proposed that *P. chinensis* var. *kissii* is more suitable as a substitute for *P. cernua* in medicinal applications.

KEGG classification analysis was conducted on the differential metabolites of the three *Pulsatilla* species, with pairwise comparisons. The results indicated that the flavonoid biosynthesis pathway had the highest degree of enrichment. Studies on plant metabolism have shown that flavonoids play a role in conferring resistance to UV-B radiation<sup>[29]</sup> and drought<sup>[30]</sup>. Notably, *Pulsatilla* species are characterized by their drought tolerance, lack of waterlogging tolerance, and preference for sunlight over shade. Therefore, the high enrichment of the flavonoid biosynthesis pathway is likely related to the growth habits of *Pulsatilla*, providing valuable insights for future research on the correlation between the growth habits and metabolites of *Pulsatilla* plants.

## Conclusions

In the three *Pulsatilla* species, the majority of triterpenoid saponin components were detected in the positive ion mode, whereas the main active components, anemoside-type triterpenoid saponins, were primarily detected in the negative ion mode. The clustering analysis results of the total metabolites across different *Pulsatilla* species from various origins revealed that environmental factors have a more significant impact than interspecies variations. Further clustering analysis of the total

differential metabolites, triterpenoid saponins, and nontriterpenoid saponins suggested that *P. chinensis* var. *kissii* is more suitable as a substitute for *P. cernua* in medicinal applications. The volcano plot of the differential metabolites showed that the main active components of *Pulsatilla*, specifically the anemoside-type components were most abundant in *P. chinensis*, followed by *P. chinensis* var. *kissii*, and least abundant in *P. cernua*. The KEGG classification of differential metabolites indicated that the flavonoid biosynthesis pathway exhibited the highest degree of enrichment among the three *Pulsatilla* species.

## Author contributions

The authors confirm contribution to the paper as follows: study conception and design: Kang T, Xu L, Zheng H; project planning and coordination: Xing Y, Yang Y; experiments performed, data analysis, draft manuscript preparation: Huang Yc, Bian C; sample preparation, targeted metabolomics analysis: Huang Yc, Huang Yt; analysis and interpretation of results: Hou W, Xue H, Huang Yc. All authors reviewed the results and approved the final version of the manuscript.

## Data availability

All data generated or analyzed during this study are included in this published article and its supplementary information files.

## Acknowledgments

This work was supported by the National Natural Science Foundation of China (Grant No. 82373999), the ability establishment of sustainable use for valuable Chinese medicine resources (Grant No. 2060302), the Liaoning Provincial Department of Education Project (JYTMS20231834), and the Liaoning Province Joint Fund (2023-MSLH-180).

## Conflict of interest

The authors declare that they have no conflict of interest.

**Supplementary information** accompanies this paper at (<https://www.maxapress.com/article/doi/10.48130/mpb-0024-0025>)

## Dates

Received 5 September 2024; Revised 12 October 2024; Accepted 16 October 2024; Published online 8 November 2024

## References

- Leng D. 2024. A comprehensive review on botany, phytochemistry, traditional uses, pharmacology, analytical methods, processing methods, pharmacokinetics and toxicity of *Pulsatilla chinensis*. *Alternative Therapies in Health and Medicine* 30(1):374–80 <https://alternative-therapies.com/oa/index.html?fid=9186>
- Editorial Committee of Chinese Pharmacopoeia CP. 2020. *Pharmacopoeia of the People's Republic of China*. Vol. 1. Beijing: China Medical Science and Technology Press. pp. 157
- Liaoning Provincial Drug Administration. 2019. *Liaoning provincial standards for Chinese medicinal materials*. Vol. 2. Shenyang: Liaoning Science and Technology Publishing House. pp. 127–28

## Metabolomics analysis

4. Jilin Provincial Drug Administration. 2020. *Jilin provincial standards for Chinese medicinal materials*. Vol. 2. Changchun: Jilin Science and Technology Publishing House. pp. 284–85
5. Mandl K. 1922. Beschreibung neuer pflanzenarten und bastarde aus ost-sibirien nebst ergänzenden bemerkungen zu wenig bekannten arten. *Österreichische Botanische Zeitschrift* 71:171–89
6. Liaoning Institute of Forestry Soils. 1975. *Flora of Herbaceous Plants in Northeast China*. Vol. 3. Beijing: Science Press. pp. 160–68
7. Editorial Committee of "Flora of China" of the Chinese Academy of Sciences. 1980. *Flora of China*. Vol. 28. Beijing: Science Press. pp. 65
8. Li YH, Zou M, Han Q, Deng LR, Weinsilboum RM. 2020. Therapeutic potential of triterpenoid saponin anemoside B4 from *Pulsatilla chinensis*. *Pharmacological Research* 160:105079
9. Kang N, Shen W, Zhang Y, Su Z, Yang S, et al. 2019. Anti-inflammatory and immune-modulatory properties of anemoside B4 isolated from *Pulsatilla chinensis* in vivo. *Phytomedicine: International Journal of Phytotherapy and Phytopharmacology* 64:152934
10. Li H, Wang L, Zhang X, Xia W, Zhou X, et al. 2022. *Pulsatilla chinensis* (bge.) regel: a systematic review on anticancer of its pharmacological properties, clinical researches and pharmacokinetic studies. *Frontiers in Oncology* 12:888075
11. Gong Q, He LL, Wang ML, Ouyang H, Gao HW, et al. 2019. Anemoside B4 protects rat kidney from adenine-induced injury by attenuating inflammation and fibrosis and enhancing podocin and nephrin expression. *Evidence-Based Complementary and Alternative Medicine: ECAM* 2019:8031039
12. Li QJ, Wang X, Wang JR, Su N, Zhang L, et al. 2019. Efficient identification of *Pulsatilla* (Ranunculaceae) using DNA barcodes and micro-morphological characters. *Frontiers in Plant Science* 10:1196
13. Liu X, Xu Y, Di J, Liu A, Jiang J. 2023. The triterpenoid saponin content difference is associated with the two type oxidosqualene cyclase gene copy numbers of *Pulsatilla chinensis* and *Pulsatilla cernua*. *Frontiers in Plant Science* 14:1144738
14. Shi Y, Zhao M, Yao H, Yang P, Xin T, et al. 2017. Rapidly discriminate commercial medicinal *Pulsatilla chinensis* (Bge.) Regel from its adulterants using ITS2 barcoding and specific PCR-RFLP assay. *Scientific Reports* 7:40000
15. Wang XR, Zhang JT, Jing WG, Li MH, Guo XH, et al. 2024. Digital identification and adulteration analysis of *Pulsatilla Radix* and *Pulsatilla Cernua* based on "digital identity" and UHPLC-QTOF-MS<sup>E</sup>. *Journal of Chromatography B* 1244:124257
16. Bian C, Xing YP, Xue HF, Hou WJ, Yang YY, et al. 2024. The complete chloroplast genome of *Pulsatilla chinensis* f. *alba* D. K. Zang (Ranunculaceae, *Pulsatilla* Miller). *Mitochondrial DNA B Resour* 9(2):233–36
17. Xiao C, Li K, Teng C, Wei Z, Li J, et al. 2023. Dietary Qi-Weng-Huangbo Powder enhances growth performance, diarrhoea and immune function of weaned piglets by modulating gut health and microbial profiles. *Frontiers in Immunology* 14:1342852
18. Fan Z, Cui Y, Chen L, Liu P, Duan W. 2024. 23-Hydroxybetulinic acid attenuates 5-fluorouracil resistance of colorectal cancer by modulating M2 macrophage polarization via STAT6 signaling. *Cancer Immunology, Immunotherapy* 73(5):83
19. Chu S, Shan D, He L, Yang S, Feng Y, et al. 2024. Anemoside B4 attenuates abdominal aortic aneurysm by limiting smooth muscle cell transdifferentiation and its mediated inflammation. *Frontiers in Immunology* 15:1412022
20. Xue M, Yang C, Huang W, He Y, Yang C, et al. 2024. Pharmacokinetics and metabolite identification of 23-hydroxybetulinic acid in rats by using liquid chromatography-mass spectrometry method. *Journal of Chromatography B* 1234:124016
21. Ye Y, Xue M, Tian X, Gao H, Hu P, et al. 2023. Pharmacokinetic and metabolite profile of orally administered anemoside B4 in rats with an improved exposure in formulations of rectal suppository. *Journal of Ethnopharmacology* 315:116694
22. Wang S, Li W, Zhang X, Li G, Li XD, et al. 2022. Metabolomics study of different germplasm resources for three *Polygonatum* species using UPLC-Q-TOF-MS/MS. *Frontiers in Plant Science* 13:826902
23. Abdelhafez OH, Othman EM, Fahim JR, Desoukey SY, Pimentel-Elardo SM, et al. 2020. Metabolomics analysis and biological investigation of three Malvaceae plants. *Phytochemical Analysis: PCA* 31(2):204–14
24. Gong X, Liu W, Cao Y, Wang R, Liang N, et al. 2022. Integrated strategy for widely targeted metabolome characterization of *Peucedani Radix*. *Journal of Chromatography A* 1678:463360
25. Li Y, Tian Y, Zhou X, Guo X, Ya H, et al. 2024. Widely targeted metabolomics reveals differences in metabolites of *Paeonia lactiflora* cultivars. *PLoS One* 19:e0298194
26. Wang Y, Liang X, Li Y, Fan Y, Li Y, et al. 2020. Changes in metabolome and nutritional quality of *Lycium barbarum* fruits from three typical growing areas of China as revealed by widely targeted metabolomics. *Metabolites* 10(2):46
27. Shang X, Huang D, Wang Y, Xiao L, Ming R, et al. 2021. Identification of nutritional ingredients and medicinal components of *Pueraria lobata* and its varieties using UPLC-MS/MS-based metabolomics. *Molecules* 26(21):6587
28. Li Y, Kong D, Fu Y, Sussman MR, Wu H. 2020. The effect of developmental and environmental factors on secondary metabolites in medicinal plants. *Plant Physiology and Biochemistry* 148:80–89
29. Liang T, Shi C, Peng Y, Tan H, Xin P, et al. 2020. Brassinosteroid-activated BRI1-EMS-SUPPRESSOR 1 inhibits flavonoid biosynthesis and coordinates growth and UV-B stress responses in plants. *The Plant Cell* 32(10):3224–39
30. Sarker U, Oba S. 2018. Drought stress enhances nutritional and bioactive compounds, phenolic acids and antioxidant capacity of *Amaranthus* leafy vegetable. *BMC Plant Biology* 18:258



Copyright: © 2024 by the author(s). Published by Maximum Academic Press, Fayetteville, GA. This article is an open access article distributed under Creative Commons Attribution License (CC BY 4.0), visit <https://creativecommons.org/licenses/by/4.0/>.